Article

Preparation of Water-Soluble Polyion Complex (PIC) Micelles Covered with Amphoteric Random Copolymer Shells with Pendant Sulfonate and Quaternary Amino Groups

Rina Nakahata and Shin-ichi Yusa *

Department of Applied Chemistry, University of Hyogo, 2167 Shosha, Himeji, Hyogo 671-2280, Japan; nkht9999@gmail.com
* Correspondence: yusa@eng.u-hyogo.ac.jp; Tel.: +81-79-267-4954

Abstract: An amphoteric random copolymer ($P(SA)_{91}$) composed of anionic sodium 2-acrylamido-2-methylpropanesulfonate (AMPS, S) and cationic 3-acrylamidopropyl trimethylammonium chloride (APTAC, A) was prepared via reversible addition-fragmentation chain transfer (RAFT) radical polymerization. The subscripts in the abbreviations indicate the degree of polymerization (DP). Furthermore, AMPS and APTAC were polymerized using a $P(SA)_{91}$ macro-chain transfer agent to prepare an anionic diblock copolymer ($P(SA)_{91}S_{67}$) and a cationic diblock copolymer ($P(SA)_{91}A_{88}$), respectively. The DP was estimated from quantitative ^{13}C NMR measurements. A stoichiometrically charge neutralized mixture of the aqueous $P(SA)_{91}S_{67}$ and $P(SA)_{91}A_{88}$ formed water-soluble polyion complex (PIC) micelles comprising PIC cores and amphoteric random copolymer shells. The PIC micelles were in a dynamic equilibrium state between PIC micelles and charge neutralized small aggregates composed of a $P(SA)_{91}S_{67}/P(SA)_{91}A_{88}$ pair. Interactions between PIC micelles and fetal bovine serum (FBS) in phosphate buffered saline (PBS) were evaluated by changing the hydrodynamic radius (R_h) and light scattering intensity (LSI). Increases in R_h and LSI were not observed for the mixture of PIC micelles and FBS in PBS for one day. This observation suggests that there is no interaction between PIC micelles and proteins, because the PIC micelle surfaces were covered with amphoteric random copolymer shells. However, with increasing time, the diblock copolymer chains that were dissociated from PIC micelles interacted with proteins.

Keywords: amphoteric random copolymer; polyelectrolyte; polyion complex; block copolymer; polymer micelle; electrostatic interaction; protein antifouling

1. Introduction

A mixture of oppositely charged polyelectrolytes in water forms a water-insoluble polyion complex (PIC) due to attractive electrostatic interactions between the polymer chains [1]. Many researchers study polymer aggregates formed by electrostatic interactions. When oppositely charged diblock copolymers containing nonionic water-soluble poly(ethylene glycol) (PEG) and polyelectrolyte blocks are mixed in water, the polymers spontaneously form water-soluble PIC micelles covered with hydrophilic PEG shells [2,3]. PIC micelles can encapsulate charged compounds such as metal ions, proteins, and nucleic acid in the PIC core via electrostatic interactions [4–11]. Recently, water-soluble PIC micelles were prepared with hydrophilic poly(2-methacryloyloxyethyl phosphorylcholine) (PMPC) coronas without net charge [12–14]. PMPC has pendant phosphorylcholine groups with the same chemical structure as the hydrophilic

part of phospholipids comprising cell membranes. The phosphorylcholine group comprises an anionic phosphonium anion and cationic quaternary amino groups. The charges in PMPC are neutralized within a single polymer chain. PMPC is a betaine polymer with good biocompatibility and antithrombogenicity [15–17].

Protein fouling on the surfaces of medical devices due to hydrophobic, electrostatic, and hydrogen bonding interactions causes deterioration of the functionality. Therefore, much attention has been given to the surface modification of medical devices using polymer coatings with antifouling properties. In general, protein antifouling polymers can bind water molecules strongly and are electrically neutral. When an antifouling polymer is coated on a substrate, proteins have minimal contact with the polymer on the substrate due to the presence of water molecules between the proteins and the polymers [18]. In particular, zwitterionic polymers can suppress protein adsorption, because they contain many bound water molecules [19]. Among these, betaine polymers effectively suppress protein adsorption [20–22]. Nanoparticles that are surface-modified with betaine polymers have an increased circulation time in the body compared to bare nanoparticles [23]. Shih et al. reported that amphoteric random copolymers with pendant anionic sulfonate and cationic quaternary amino groups inhibit protein adsorption for stoichiometrically charge neutralized compositions [24]. It is expected that amphoteric random copolymers can be applied to the surface modification of medical devices.

In the present study, we prepared an amphoteric random copolymer $(P(SA)_{91})$ macro chain transfer agent (CTA) composed of the same amounts of anionic sodium 2-acrylamido-2-methylpropanesulfonate (AMPS, S) and cationic 3-acrylamidopropyl trimethylammonium chloride (APTAC, A) via reversible addition-fragmentation chain transfer (RAFT) radical polymerization [25]. AMPS and APTAC were polymerized using $P(SA)_{91}$ macro-CTA to prepare an anionic diblock copolymer $(P(SA)_{91}S_{67})$ and a cationic diblock copolymer $(P(SA)_{91}A_{88})$, respectively (Figure 1). The subscripts in the abbreviations indicate the degree of polymerization (DP). Water-soluble PIC micelles were prepared by stoichiometrically charge neutralized mixing of the oppositely charged diblock copolymers, $P(SA)_{91}S_{67}$ and $P(SA)_{91}A_{88}$, in water. To the best of our knowledge, this is the first report on such micelles. The PIC micelles inhibit interactions with proteins, because their surface is covered with amphoteric random $P(SA)_{91}$ copolymer shells.
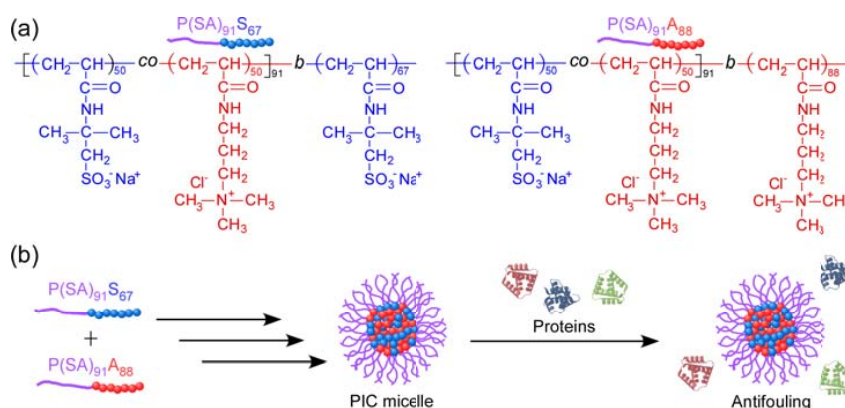

Figure 1. (**a**) Chemical structures of $P(SA)_{91}S_{67}$ and $P(SA)_{91}A_{88}$. (**b**) Schematic representation of water-soluble polyion complex (PIC) micelle formed from a mixture of $P(SA)_{91}S_{67}$ and $P(SA)_{91}A_{88}$; the PIC micelle shows protein antifouling properties because of its amphoteric random copolymer shell.

2. Materials and Methods

2.1. Materials

2-Acrylamido-2-methylpropanesulfonic acid (AMPS, 98%) from Tokyo Chemical Industry (Tokyo, Japan) and 4,4′-azobis(4-cyanopentanoic acid) (V-501, 98%) from Wako Pure Chemical

(Osaka, Japan) were used as received without further purification, and 3-acrylamidopropyl trimethylammonium chloride (APTAC, 75 wt % in water) from Tokyo Chemical Industry was passed through an Aldrich (St Louis, MO, USA) disposable inhibitor removal column. Methanol was dried with molecular sieves 3A and purified by distillation. Phosphate buffered saline (PBS) was prepared by dissolving one PBS tablet (Aldrich) in predetermined amounts of water, while 4-cyanopentanoic acid dithiobenzoate (CPD) was synthesized according to a reported method [26]. Bovine serum albumin (BSA, pH 5.0–5.6 solution) from Wako Pure Chemical and fetal bovine serum (FBS) from GE Healthcare Life Sciences HyClone were used without further purification. Water was purified using an ion-exchange column. Other reagents were used as received.

2.2. Preparation of P(SA)$_{91}$

AMPS (10.0 g, 48.3 mmol) was neutralized with 6 M aqueous NaOH (10.9 mL) to adjust the pH to 6.0. APTAC (9.98 g, 48.3 mmol), V-501 (135 mg, 0.482 mmol), and CPD (270 mg, 0.965 mmol) were dissolved in a mixed solvent of MeOH (5 mL) and water (32 mL), which was added to the aqueous AMPS. The solution was degassed by purging with Ar for 30 min. Polymerization was carried out at 70 °C for 24 h. After the reaction, the total conversion of AMPS and APTAC estimated from ^{1}H NMR was 90.9%. The reaction mixture was dialyzed against 1.5 M aqueous NaCl for one day, and then pure water for one day using a dialysis membrane with a molecular weight cutoff of 14 kDa (EIDIA Co. Ltd, Tokyo, Japan). The polymer (P(SA)$_{91}$) was recovered by a freeze-drying technique (15.3 g, 71.8%). The theoretical degree of polymerization (DP(theory)) and number-average molecular weight (M_n(theory)) were 91 and 1.91×10^4 g/mol, respectively, estimated from the conversion and molar ratio of monomer to CPD (Formulars 1 and 2). The number-average molecular weight (M_n(GPC)) and molecular weight distribution (M_w/M_n) were 1.54×10^4 g/mol and 1.27, respectively, estimated from gel-permeation chromatography (GPC). The APTAC content was 50 mol%, estimated from quantitative ^{13}C NMR measurements. The synthesis route of P(SA)$_{91}$ is shown in Figure S1.

2.3. Preparation of P(SA)$_{91}$S$_{67}$

AMPS (771 mg, 3.72 mmol) was neutralized with 6 M aqueous NaOH (6.2 mL) to adjust the pH to 6.0. P(SA)$_{91}$ (703 mg, 3.68×10^{-2} mmol, M_n(theory) = 1.91×10^4 g/mol, M_w/M_n = 1.27) and V−501 (4.15 mg, 1.48×10^{-2} mmol) were added to the aqueous solution. The solution was degassed by purging with Ar for 30 min. Polymerization was carried out at 70 °C for 24 h (conversion = 90.9%). The reaction mixture was dialyzed against 1.5 M aqueous NaCl for one day, and then pure water for one day. The polymer (P(SA)$_{91}$S$_{67}$) was recovered by a freeze-drying technique (1.23 g, 67.6%). The degree of polymerization (DP(NMR)) of the PAMPS block was 67, estimated from quantitative ^{13}C NMR measurements. M_n(GPC) and M_w/M_n were 2.38×10^4 g/mol and 1.04, respectively, estimated from GPC. The synthesis route of P(SA)$_{91}$S$_{67}$ is shown in Figure S1.

2.4. Preparation of P(SA)$_{91}$A$_{88}$

APTAC (765 mg, 3.69 mmol), P(SA)$_{91}$ (703 mg, 3.68×10^{-2} mmol, M_n(theory) = 1.91×10^4 g/mol, M_w/M_n = 1.27), and V-501 (4.14 mg, 1.48×10^{-2} mmol) were dissolved in water (7.1 mL). The solution was degassed by purging with Ar for 30 min. Polymerization was carried out at 70 °C for 24 h (conversion = 87.7%). The reaction mixture was dialyzed against 1.5 M aqueous NaCl for one day, and then pure water for one day. The polymer (P(SA)$_{91}$A$_{88}$) was recovered by a freeze-drying technique (1.10 g, 74.9%). The DP(NMR) of the PAPTAC block was 88, estimated from quantitative ^{13}C NMR measurements. M_n(GPC) and M_w/M_n were 1.87×10^4 g/mol and 1.14, respectively, estimated from GPC. The synthesis route of P(SA)$_{91}$A$_{88}$ is shown in Figure S1.

2.5. Preparation of PIC micelles

P(SA)$_{91}$S$_{67}$ and P(SA)$_{91}$A$_{88}$ were dissolved separately in 0.1 M aqueous NaCl. The aqueous P(SA)$_{91}$A$_{88}$ was added to the P(SA)$_{91}$S$_{67}$ solution over a period of 5 min with stirring to prepare the

PIC micelles. The mixing ratio of the polymers was represented by the molar fraction of cationic charge (f^+ = [APTAC]/([AMPS] + [APTAC])). The PIC micelles were prepared at f^+ = 0.5 unless otherwise noted, which represents complete charge neutralization.

2.6. Measurements

The ^{1}H NMR and inverse-gated decoupling ^{13}C NMR spectra were obtained in D_2O using a Bruker (Yokohma, Japan) DRX-500 spectrometer. GPC measurements were performed using a Jasco (Tokyo, Japan)UV-2075 detector equipped with a Shodex (Tokyo, Japan) OHpak SB-804 HQ column working at 40 °C with a flow rate of 0.6 mL/min. An acetic acid (0.5 M) solution containing sodium sulfate (0.3 M) was used as the eluent. Sample solutions were filtered with a 0.2 μm pore size membrane filter. M_n and M_w/M_n for the polymers were calibrated using standard poly(2-vinylpyridine) (P2VP) samples. Dynamic light scattering (DLS) measurements were obtained using a Malvern (Worcestershire, UK) Zetasizer Nano ZS with a He-Ne laser (4 mW at 633 nm) at 25 °C. The hydrodynamic radius (R_h) was calculated using the Stokes-Einstein equation, $R_h = k_BT/(6\pi\eta D)$, where k_B is the Boltzmann constant, T is the absolute temperature, and η is the solvent viscosity. The DLS data was analyzed using Malvern Zetasizer software version 7.11. The angular dependence of DLS and static light scattering (SLS) was measured using an Otsuka Electronics Photal (Osaka, Japan) DLS-7000HL light scattering spectrometer equipped with a multi-τ digital time correlator (ALV-5000E), at 25 °C. A He-Ne laser (10 mW at 633 nm) was used as the light source [27–29]. The weight-average molecular weight (M_w), z-average radius of gyration (R_g), and second virial coefficient (A_2) were estimated from SLS measurements [30]. Sample solutions for light scattering measurements were filtered using a membrane filter with 0.2 μm pores. The known Rayleigh ratio of toluene was used to calibrate the instrument. Plots of the refractive index increments against polymer concentration (dn/dC_p) at 633 nm were obtained with an Otsuka Electronics Photal DRM-3000 differential refractometer at 25 °C. The zeta potential was measured using a Malvern Zetasizer Nano-ZS equipped with a He-Ne laser light source (4 mW, at 632.8 nm) at 25 °C. The zeta potential (ζ) was calculated from the electrophoretic mobility (μ) using the Smoluchowski relationship, $\zeta = \eta\mu/\varepsilon$ ($\kappa a \gg 1$), where η is the viscosity of the solvent, ε is the dielectric constant of the solvent, and κ and a are the Debye-Hückel parameter and particle radius, respectively [31]. TEM was performed with a JEOL (Tokyo, Japan) JEM-2100 microscope at an accelerating voltage of 200 kV. A sample for TEM was prepared by placing one drop of the aqueous solution on a copper grid coated with a thin film of Formvar. Excess water was blotted using filter paper. The sample was stained with sodium phosphotungstate and dried under vacuum for one day.

3. Results and Discussion

3.1. Preparation of $P(SA)_{91}S_{67}$ and $P(SA)_{91}A_{88}$

The monomer conversions (p) of AMPS and APTAC could not be determined individually from ^{1}H NMR measurements, because the peaks of vinyl groups in the monomers completely overlapped around 5.5–6.5 ppm. The sum of p for the AMPS and APTAC monomers was estimated from the integral intensity ratio of the vinyl groups compared to the sum of AMPS and APTAC pendant methylene protons at 3.0–3.5 ppm after polymerization. The monomer reactivity ratios for AMPS and APTAC are assumed to be one, because the polymerizable functional groups had the same chemical structure, i.e., acrylamide-type. When random copolymerization was performed to prepare $P(SA)_{91}$ with equal concentrations of AMPS ($[M_{AMPS}]_0$) and APTAC ($[M_{APTAC}]_0$), DP(theory) and M_n(theory) were calculated from the following formulas:

$$\text{DP(theory)} = \frac{2[M_{AMPS}]_0}{[CTA]_0} \times \frac{p}{100} \tag{1}$$

$$M_n(\text{theory}) = \text{DP(theory)} \times \text{MW}_{MAV} + \text{MW}_{CTA} \tag{2}$$

where $[CTA]_0$ is the initial concentration of CTA, MW_{MAV} is the average molecular weight of AMPS and APTAC, and MW_{CTA} is the molecular weight of CTA. When $[M_{AMPS}]_0 = [M_{APTAC}]_0$, the total monomer concentration becomes $2[M_{AMPS}]_0$. The values of DP(theory) and M_n(theory) are listed in Table 1.

Table 1. Degree of polymerization (DP), number-average molecular weight (M_n), and molecular weight distribution (M_n/M_n).

Sample	DP (theory) [a]	M_n(theory) [b] $\times 10^4$ (g/mol)	DP (NMR) [c]	M_n(NMR) $\times 10^4$ (g/mol)	M_n(GPC) $\times 10^4$ (g/mol)	M_w/M_n
P(SA)$_{91}$	91	1.91	$-$ [d]	$-$ [d]	1.54	1.27
P(SA)$_{91}$S$_{67}$	61	3.30	67	3.27	2.38	1.04
P(SA)$_{91}$A$_{88}$	90	3.73	88	3.70	1.87	1.15

[a] Theoretical degree of polymerization estimated from Formula 1. [b] Theoretical number-average molecular weight estimated from Formula 2. [c] Estimated from quantitative inverse-gated decoupling ^{13}C NMR spectra in D_2O. [d] The values could not be determined from ^{1}H NMR, because the terminal phenyl protons overlapped with the pendant amino protons.

The composition of P(SA)$_{91}$ could not be determined from ^{1}H NMR, because the peaks of the AMPS and APTAC units overlapped (Figure S2). To determine the compositions of P(SA)$_{91}$, quantitative inverse gated decoupling ^{13}C NMR measurements were performed in D_2O (Figure 2a). The contents of AMPS and APTAC in the amphoteric random copolymer were determined from the integral intensity ratio of the peaks at 57.6 and 64.2 ppm, attributed to the pendant methylene carbons in AMPS and APTAC, respectively. The compositions of AMPS and APTAC in P(SA)$_{91}$ were both 50 mol %. The DP(NMR) values for the PAMPS and PAPTAC blocks in P(SA)$_{91}$S$_{67}$ and P(SA)$_{91}$A$_{88}$ were found to be 67 and 88, respectively, using quantitative ^{13}C NMR measurements (Figure 2b,c). The M_n(NMR) values for P(SA)$_{91}$S$_{67}$ and P(SA)$_{91}$A$_{88}$ were close to the M_n(theory) values. However, the M_n(GPC) values for P(SA)$_{91}$S$_{67}$ and P(SA)$_{91}$A$_{88}$ deviated from the theoretical values, which indicates that there are interactions between the sample polymers and that the GPC column or the GPC standard sample (P2VP) was unsuitable for determining M_n(GPC) (Figure S3). The M_w/M_n values for P(SA)$_{91}$S$_{67}$ and P(SA)$_{91}$A$_{88}$ were relatively small (1.04–1.15), which suggests that the obtained polymers have well-controlled structures.
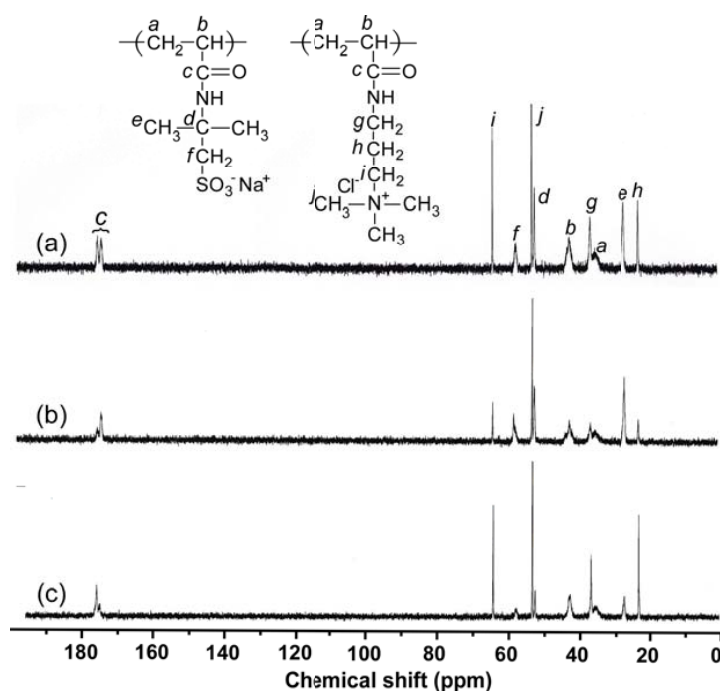
Figure 2. Inverse gated decoupling ^{13}C NMR spectra of (**a**) $P(SA)_{91}$, (**b**) $P(SA)_{91}S_{67}$, and (**c**) $P(SA)_{91}A_{88}$ in D_2O.

3.2. Preparation and Characterization of PIC Micelles

The R_h values for $P(SA)_{91}S_{67}$ and $P(SA)_{91}A_{88}$ in 0.1 M aqueous NaCl were 5.7 and 6.0 nm, respectively (Figure 3). These had unimodal distributions. The polydispersity indices (PDI) for $P(SA)_{91}S_{67}$ and $P(SA)_{91}A_{88}$ were 0.147–0.169. The R_h for the stoichiometrically charge neutralized mixture of $P(SA)_{91}S_{67}$ and $P(SA)_{91}A_{88}$ increased to 29.0 nm, which suggests the formation of PIC micelles. Assuming that the polymer main chain has a planar zig-zag structure, the expanded chain lengths of $P(SA)_{91}S_{67}$ and $P(SA)_{91}A_{88}$ are 39.5 and 44.8 nm, respectively. These are longer than the R_h of the PIC micelles (= 29.0 nm). This suggests that a PIC micelle has a simple spherical core-shell structure composed of a core formed from the anionic PAMPS and cationic PAPTAC blocks and an amphoteric $P(SA)_{91}$ shell. The PDI for PIC micelles was narrower than for $P(SA)_{91}S_{67}$ and $P(SA)_{91}A_{88}$, which indicates that the PIC micelles have a uniform size.

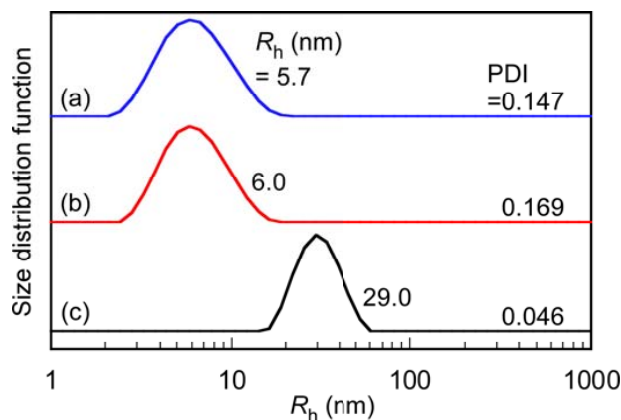**Figure 3.** Hydrodynamic radius (R_h) distributions with polydispersity indices (PDI) for (**a**) $P(SA)_{91}S_{67}$; (**b**) $P(SA)_{91}A_{88}$; and (**c**) PIC micelles in 0.1 M aqueous NaCl.

The relationship between the relaxation rate (Γ) and light scattering angle (θ) was measured for PIC micelles in 0.1 M aqueous NaCl (Figure S4). The scattering vector (q) was calculated using $q = (4\pi n/\lambda)\sin(\theta/2)$, where n is the refractive index of the solvent and λ is the wavelength of the light source (= 632.8 nm). The Γ-q^2 plot was a straight line passing through the origin. Therefore, R_h was determined at $\theta = 90°$, because the diffusion coefficient (D) was independent of θ.

The R_h, LSI, and zeta potential for the mixture of P(SA)$_{91}$S$_{67}$ and P(SA)$_{91}$A$_{88}$ at various f^+ were measured in 0.1 M aqueous NaCl (Figure 4). The total polymer concentration in the solution was maintained at 1.0 g/L. We performed the LSI and zeta-potential experiments at $f^+ = 0$ and 1 were performed at $C_p = 10.0$ g/L, because LSIs were too low to measure R_h and zeta-potential. The compensated LSIs at $f^+ = 0$ and 1 are plotted in Figure 4a. At $f^+ = 0$, the values indicated for aqueous P(SA)$_{91}$S$_{67}$, and the zeta potential was –11.4 mV due to the negative charge of the PAMPS block. At $f^+ = 1$, the zeta potential for P(SA)$_{91}$A$_{88}$ was 8.40 mV due to the positive charge of the PAPTAC block. The zeta potential of the stoichiometrically charge neutralized mixture of P(SA)$_{91}$S$_{67}$ and P(SA)$_{91}$A$_{88}$ at $f^+ = 0.5$ was close to 0 mV. At $f^+ = 0.5$, the R_h and LSI had the highest values for PIC micelles. We will discuss the structure of PIC micelles in more detail, together with the results of the DLS, SLS, and TEM measurements, later in this paper.
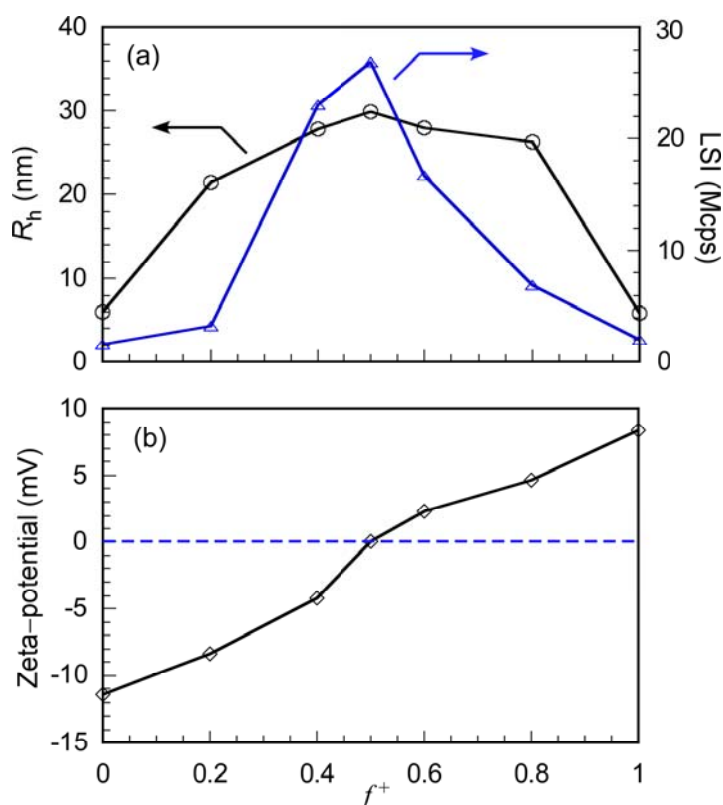

Figure 4. (**a**) Hydrodynamic radius (R_h, ○) and light scattering intensity (LSI, △) of PIC micelles as a function of f^+ (= [APTAC]/([APTAC] + [AMPS])) in 0.1 M aqueous NaCl; (**b**) Zeta potential of PIC micelles as a function of f^+ in 0.1 M aqueous NaCl.

The R_h and LSI of PC micelles were plotted against C_p (Figure S5). R_h remained almost constant at about 30 nm and was independent of C_p in the range $0.02 \leq C_p \leq 1.0$ g/L. LSI increased linearly with C_p. These observations suggest that the shape and aggregation number (N_{agg}), which is the number of polymer chains that form one PIC micelle, may be constant and independent of C_p in this region (0.02–1.0 g/L). At $C_p \leq 0.02$ g/L, the LSI for PIC micelles was too low to obtain R_h. We studied

the time dependence on R_h and LSI for PIC micelles. The R_h and LSI values remained constant until at least 41 h (Figure S6).

Table 2. Dynamic light scattering (DLS) and static light scattering (SLS) data for $P(SA)_{91}S_{67}$, $P(SA)_{91}A_{88}$, and PIC micelles in 0.1 M NaCl.

Samples	$M_w \times 10^4$ (g/mol)	N_{agg}	R_g (nm)	R_h (nm)	R_g/R_h	$A_2 \times 10^{-4}$ (cm³·mol/g²)	d [a] (g/cm³)	dn/dC_p (mL/g)
$P(SA)_{91}S_{67}$	5.41	1	7.3	5.7	1.28	3.73	0.116	0.118
$P(SA)_{91}A_{88}$	4.98	1	6.7	6.0	1.12	3.77	0.0914	0.138
PIC micelles	752	218	26.5	29.0	0.91	0.0127	0.122	0.128

[a] Estimated from the values of M_w and R_h using Formula 3.

SLS measurements for $P(SA)_{91}S_{67}$, $P(SA)_{91}A_{88}$, and PIC micelles were performed in 0.1 M aqueous NaCl (Table 2). M_w was estimated by extrapolating C_p and θ to zero in Zimm plots (Figure S7). R_g was estimated from the slope of θ at $C_p \to 0$. A_2 was estimated from the slope of C_p at $\theta \to 0$. The N_{agg} of the PIC micelles was 218, as calculated from the M_w ratio of the PIC micelles and the unimer states of $P(SA)_{91}S_{67}$ and $P(SA)_{91}A_{88}$. The M_w values of the unimer states of the block copolymers estimated from SLS were close to the weight-average molecular weight calculated from M_n(NMR) and M_w/M_n (Table 1). R_g/R_h is useful for determining the shape of molecular aggregates. The theoretical value of R_g/R_h for a homogeneous hard sphere is 0.778, while that of a random coil is about 1, and this increases substantially for a structure with a lower density and polydispersity, e.g., R_g/R_h = 1.5–1.7 for flexible linear chains, and $R_g/R_h \geq 2$ for a rod [32]. The PIC micelles may be spherical, because R_g/R_h = 0.91, which is close to 1. The R_g/R_h ratios for $P(SA)_{91}S_{67}$ and $P(SA)_{91}A_{88}$ were above 1, which suggests that the block copolymer chains were relatively expanded due to electrostatic repulsions in the polyelectrolyte blocks in 0.1 M aqueous NaCl. In general, A_2 relates to the interactions between a polymer chain and solvent. A large value of A_2 indicates a good solvent; however, a small or negative value of A_2 indicates a poor solvent [33,34]. For the PIC micelles, A_2 was 1.27×10^{-6} cm³·mol/g, which was less than the corresponding values for $P(SA)_{91}S_{67}$ and $P(SA)_{91}A_{88}$ (3.73×10^{-4} and 3.77×10^{-4} cm³·mol/g). This indicates that the solubility of PIC micelles in 0.1 M NaCl decreased compared with those of the unimer states of the block copolymers because of the insoluble PIC core in the PIC micelles. The density (d) for $P(SA)_{91}S_{67}$, $P(SA)_{91}A_{88}$, and PIC micelles was calculated using the following formula:

$$d = \frac{M_w}{N_A \times V} \tag{2}$$

where V is the volume of the block copolymers or PIC micelles calculated from $4/3\pi R_h^3$. The d values for $P(SA)_{91}S_{67}$ and $P(SA)_{91}A_{88}$ were 0.116 and 0.0914 g/cm³, respectively, while d was 0.122 g/cm³ for the PIC micelles, which was slightly larger than for the diblock copolymers in the unimer states. This suggests that the polymer chains in the PIC micelles were more densely packed than those in the unimer states, because the PIC micelle core was formed by strong electrostatic interactions.

TEM was performed on PIC micelles in 0.1 M aqueous NaCl (Figure 5). The average radius of a PIC micelle was 20.3 nm, estimated from TEM, which was smaller than R_h (= 29.0 nm) estimated from DLS, because the TEM sample was in the dry state. Recently, we have reported the solution properties of amphoteric random copolymers in aqueous solutions [25]. We found out that there are no interpolymer interactions of amphoteric random copolymers in 0.1 M NaCl aqueous solutions. Also, we confirmed that there are on interactions between $P(SA)_{91}$ and anionic and cationic homopolymers using DLS measurements. From these findings, there are no interactions between amphoteric random copolymer shells in PIC micelles. Moreover, there are no interactions between amphoteric random copolymer shells and the PIC core. The PIC micelle system has the same chemical structure in the core and corona, as both domains have the same composition [35].
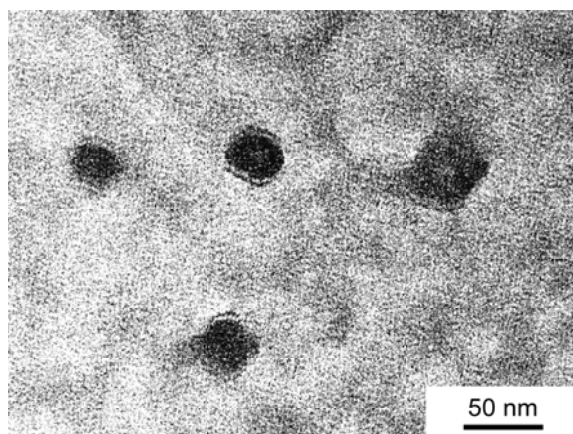
Figure 5. TEM image of PIC micelles with f^+ = 0.5 at C_p = 1.0 g/L in 0.1 M aqueous NaCl.

The critical micelle concentration (cmc) for PIC micelles in 0.1 M aqueous NaCl was determined from the relationship between the LSI ratio (I/I_0) and C_p (Figure 6). I and I_0 are the LSIs of the solution and solvent, respectively. Although R_h for the PIC micelles cannot be measured for $C_p \leq 0.02$ g/L, I/I_0 can be measured below 0.02 g/L. The crossing point of the linear portions in the low and high C_p regions was 0.002 g/L, as the cmc. Below the cmc, PIC micelles may dissociate into charge neutralized small aggregates composed of a P(SA)$_{91}$S$_{67}$/P(SA)$_{91}$A$_{88}$ pair [36]. PIC micelles thus have a cmc, suggesting that they are in a dynamic equilibrium state.
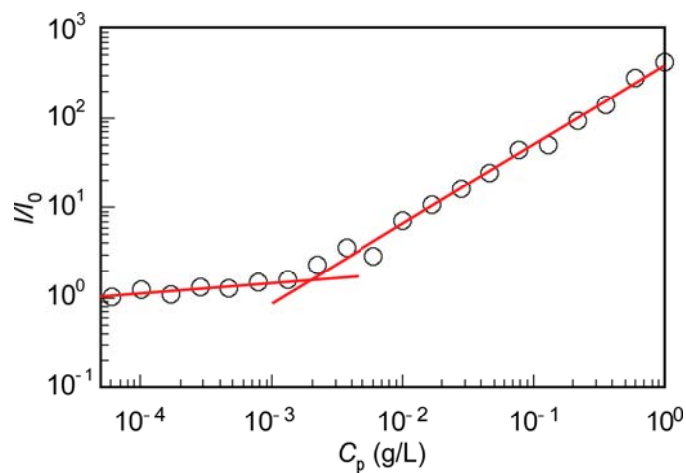
Figure 6. Light scattering intensity ratio (I/I_0) for the aqueous PIC micelles containing 0.1 M NaCl as a function of polymer concentration (C_p). I and I_0 are the light scattering intensities of the solution and solvent, respectively.

PIC micelles formed due to electrostatic interactions of the anionic and cationic blocks. When a low molecular weight salt such as NaCl is added to aqueous PIC micelles, their shape may change because of a screening effect [37,38]. R_h and LSI for the aqueous PIC micelles were plotted as a function of the NaCl concentration ([NaCl]) (Figure 7). At [NaCl] $\leq$ 0.7 M, R_h gradually decreased with increasing [NaCl], and R_h was 25.8 nm at [NaCl] = 0.7 M. R_h decreased rapidly at 0.7 M < [NaCl] $\leq$ 0.8 M, and R_h was about 12 nm at [NaCl] = 0.8 M. The LSI decreased almost monotonously with increasing [NaCl] until [NaCl] = 0.8 M. At [NaCl] > 0.8 M, the LSI was almost constant and independent of [NaCl]. This observation indicates that the PIC micelles partially dissociated due to the screening effect of NaCl. R_h was almost constant at 9–12 nm at [NaCl] > 0.8 M. The R_h values for the unimer states of P(SA)$_{91}$S$_{67}$

and P(SA)$_{91}$A$_{88}$ were 5.7–6.0 nm (Figure 3). The R_h values for PIC micelles at [NaCl] > 0.8 M were larger than those for the unimer states. These observations suggest that PIC micelles cannot dissociate into their unimer states at [NaCl] > 0.8 M, presumably because of salting out effects.
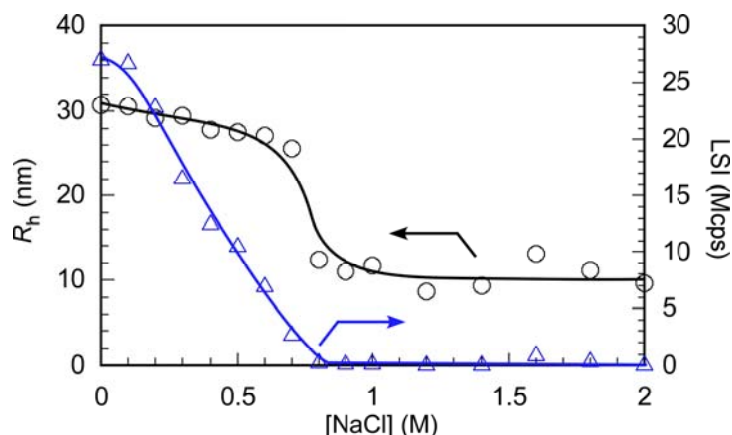

Figure 7. Hydrodynamic radius (R_h, ○) and light scattering intensity (LSI, △) of PIC micelles with f^+ = 0.5 at C_p = 1.0 g/L as a function of NaCl concentration ([NaCl]).

3.3. Interactions between PIC Micelles and Proteins

We evaluated the interactions between PIC micelles (0.1 g/L) and BSA (5.0 g/L) in PBS using DLS (Figure 8). Before mixing, the R_h distributions were unimodal, and the R_h values for PIC micelles and BSA were 29.0 and 4.9 nm, respectively. A mixed solution of PIC micelles and BSA was prepared in PBS, and then DLS was performed on the solution within 1 h. After mixing, the distribution became bimodal, with R_h = 5.1 and 31.5 nm. The R_h value of the large size distribution was close to the R_h (= 29.0 nm) of the PIC micelles. Before mixing, the LSI values for the PIC micelles and BSA were 1.9 and 2.0 Mcps, respectively. The LSI for the mixture of PIC micelles and BSA was 2.1 Mcps, which was close to the values before mixing. This indicates that the PIC micelles do not interact considerably with BSA.
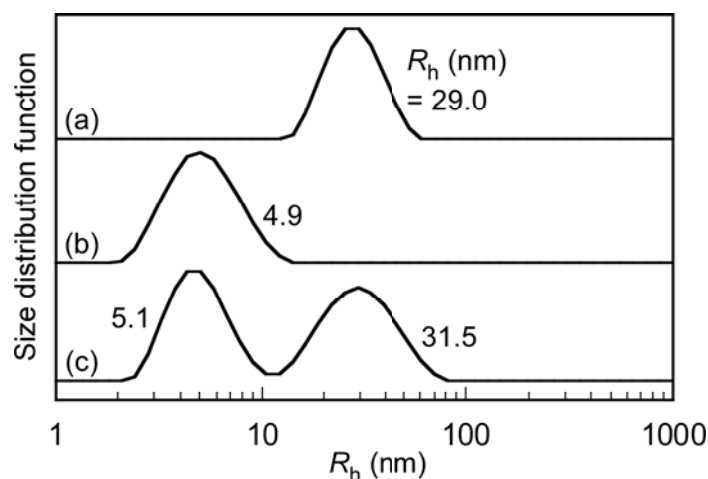

Figure 8. R_h distributions of (**a**) PIC micelles; (**b**) BSA; and (**c**) a mixture of PIC micelles with BSA in PBS at 25 °C.

The time dependences of R_h and LSI for the mixture of PIC micelles and BSA were determined (Figure S8). The R_h distributions and LSI remained almost constant for one day. After two days, the distribution became trimodal. A small third distribution peak with an R_h of about 200 nm was

observed after two days. The large aggregates with $R_h \geq 200$ nm may be formed from BSA and unit PIC of a pair of $P(SA)_{91}S_{67}/P(SA)_{91}A_{88}$ dissociated from the PIC micelles. After four days, the area of the third distribution peak increased, and R_h increased to 281 nm. The average R_h and LSI for the mixture were almost constant for three days; however, these increased after four days. These observations suggest that the interaction between PIC micelles and proteins increased with time. The block copolymer chains can dissociate from the PIC micelles because these are in a dynamic equilibrium state. The unit PICs of $P(SA)_{91}S_{67}/P(SA)_{91}A_{88}$ detached from the PIC micelles may interact with proteins due to electrostatic attractions. The total charges in the unit PIC are compensated. However, dangling charge loops may be formed in the complex of cationic PAMPTAC and anionic PAMSP blocks in the unit PIC (Figure S9). In the case of PIC micelles, the surface of the PIC core was completely covered with amphoteric random copolymer shells which have protein antifouling properties. On the other hand, in the case of the unit PIC, the dangling charge loops may be exposed. The dangling charge groups in the unit PIC strongly interacted with proteins to form large aggregates.

The interactions between PIC micelles (0.1 g/L) and FBS (40 g/L) in PBS were evaluated by DLS (Figure 9). While BSA is a negatively charged protein, FBS is a mixture of negatively and positively charged proteins. The R_h distribution for FBS was bimodal with R_h = 5.3 and 31.8 nm. Mixed PBS solutions of PIC micelles and FBS were prepared, and then DLS was performed within 1 h. The R_h values for the mixture of PIC micelles and FBS were similar to those for FBS. The LSI of the mixed solution was 2.1 Mcps, which was similar to the values for the PIC micelles (1.9 Mcps) and FBS (2.1 Mcps) before mixing. This indicates that there is no interaction between PIC micelles and FBS. The time dependences of R_h distributions for the mixture of PIC micelles and FBS were measured (Figure S10). After two days, the distribution became trimodal. A small third distribution peak with an R_h of about 200 nm was observed after two days, which suggests that the large aggregates were formed from FBS and unit PIC formed.
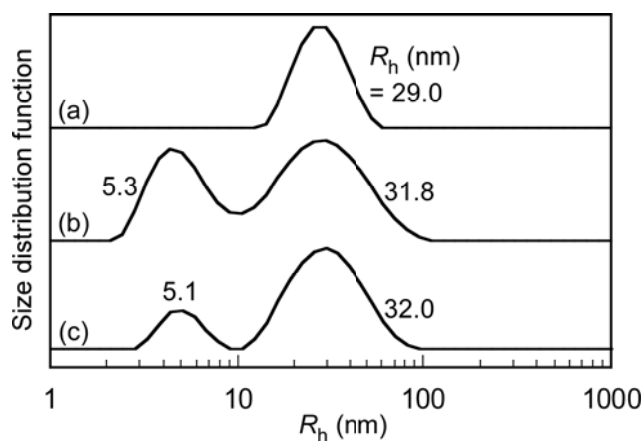

Figure 9. (a) R_h distributions for (**a**) PIC micelles, (**b**) FBS, and (**c**) a mixture of PIC micelles with FBS in PBS buffer at 25 °C.

4. Conclusions

Oppositely charged diblock copolymers of anionic $P(SA)_{91}S_{67}$ and cationic $P(SA)_{91}A_{88}$ were prepared via RAFT using $P(SA)_{91}$ macro-CTA. Water-soluble PIC micelles were formed from a stoichiometrically charge neutralized mixture of 0.1 M aqueous NaCl solutions of $P(SA)_{91}S_{67}$ and $P(SA)_{91}A_{88}$. The maximum values of R_h and LSI were observed when f^+ was 0.5, and the zeta potential was close to 0 mV. The PIC micelles were in a dynamic equilibrium state with PIC micelles and charge neutralized small aggregates composed of a $P(SA)_{91}S_{67}/P(SA)_{91}A_{88}$ pair. The particle sizes in the mixture of PIC micelles and proteins in PBS remained almost constant for at least one day, which suggests that there is no interaction between PIC micelles and proteins. The PIC micelles were

covered with amphoteric $P(SA)_{91}$ shells that suppressed their interaction with proteins. However, the interactions of the diblock copolymer chains dissociated from PIC micelles and proteins increased with time. If the lengths of the PAMPS block in $P(SA)_{91}S_{67}$ and the PAPTSC block in $P(SA)_{91}A_{88}$ increased, the dynamic equilibrium may shift to form PIC micelles. Therefore, it is expected that the interaction of PIC micelles with long polyelectrolyte chains and proteins can be suppressed for a long time.

Supplementary Materials: The following are available online at http://www.mdpi.com/2073-4360/10/2/205/s1; Figure S1: Synthesis routes of $P(SA)_{91}S_{67}$ and $P(SA)_{91}A_{88}$; Figure S2: ^{1}H NMR spectra for (a) $P(SA)_{91}$, (b) $P(SA)_{91}S_{67}$, and (c) $P(SA)_{91}A_{88}$ in D_2O; Figure S3: GPC elution curves for (a) $P(SA)_{91}S_{67}$ and (b) $P(SA)_{91}A_{88}$ using an acetic acid (0.5 M) solution containing sodium sulfate (0.3 M) as an eluent; Figure S4: Relationship between the relaxation rate (Γ) and the square of the magnitude of the scattering intensity vector (q^2) for PIC micelles at $C_p = 1$ g/L in 0.1 M aqueous NaCl at 25 °C; Figure S5: Hydrodynamic radius (R_h, ○) and light scattering intensity (LSI, △) of PIC micelles as a function of polymer concentration (C_p) in 0.1 M aqueous NaCl. Figure S6: Relationship between R_h (○) and light scattering intensity (LSI, △) as a function of time for PIC micelle with $f^+ = 0.5$ at $C_p = 1.0$ g/L in 0.1 M NaCl aqueous solution; Figure S7: A typical Zimm plot for PIC micelles in 0.1 M aqueous NaCl at 25 °C; Figure S8: (a) Relationship between R_h (○) and light scattering intensity (LSI, △) as a function of time, and (b) R_h distributions for a mixture of PIC micelles/BSA at $C_p = 0.1$ g/L and [BSA] = 5.0 g/L in PBS at 25 °C; Figure S9: Conceptual illustration of dangling charge groups in the unit PIC of $P(SA)_{91}S_{67}/P(SA)_{91}A_{88}$; Figure S10: R_h distributions for mixture of PIC micelle/FBS at $C_p = 0.1$ g/L and [FBS] = 40 g/L in PBS at 25 °C.

Author Contributions: Rina Nakahata was a research student who performed the experimental work. Shin-ichi Yusa was responsible for analyzing the experimental data and writing the paper. All authors approved the manuscript.

Conflicts of Interest: The authors declare no conflict of interest.

References

1. Michaels, A.S.; Miekka, R.G. Polycation-polyanion complexes: preparation and properties of poly(vinylbenzyltrimethylammonium) poly(styrensulfonate). *J. Phys. Chem.* **1961**, *65*, 1765–1773. [CrossRef]
2. Wibowo, A.; Osada, K.; Matsuda, H.; Anraku, Y.; Hirose, H.; Kishimura, A.; Kataoka, K. Morphology control in water of polyion complex nanoarchitectures of double-hydrophilic charged block copolymers through composition tuning and thermal treatment. *Macromolecules* **2014**, *47*, 3086–3092. [CrossRef]
3. Yusa, S.; Yokoyama, Y.; Morishima, Y. Synthesis of oppositely charged block copolymers of poly(ethylene glycol) via reversible addition–fragmentation chain transfer (RAFT) radical polymerization and characterization of their polyion complex (PIC) micelles in water. *Macromolecules* **2009**, *42*, 376–383. [CrossRef]
4. Oparin, A.I. Origin and evolution of metabolism. *Comp. Biochem. Physiol.* **1962**, *4*, 371–377. [CrossRef]
5. Oishi, M.; Nagasaki, Y.; Itaka, K.; Nishiyama, N.; Kataoka, K. Lactosylated poly(ethylene glycol)-siRNA conjugate through acid-labile β-thiopropionate linkage to construct pH-sensitive polyion complex micelles achieving enhanced gene silencing in hepatoma cells. *J. Am. Chem. Soc.* **2005**, *127*, 1624–1625. [CrossRef] [PubMed]
6. Van der Gucht, J.; Spruijt, E.; Lemmers, M.; Cohen Stuart, M.A. Polyelectrolyte complexes: Bulk phases and colloidal systems. *J. Colloid Interface Sci.* **2011**, *361*, 407–422. [CrossRef] [PubMed]
7. Müller, M. Sizing, shaping and pharmaceutical applications of polyelectrolyte complex nanoparticles. *Adv. Polym. Sci.* **2014**, *256*, 197–260.
8. Pergushov, D.V.; Mueller, A.H.; Schacher, F.H. Micellar interpolyelectrolyte complexes. *Chem. Soc. Rev.* **2012**, *41*, 6888–6901. [CrossRef] [PubMed]
9. Voets, I.K.; de Keizer, A.; Stuart, M.A.C. Complex coacervate core micelles. *Adv. Colloid Interface Sci.* **2009**, *147*, 300–318. [CrossRef] [PubMed]
10. Steinschulte, A.A.; Gelissen, A.P.H.; Jung, A.; Brugnoni, M.; Caumanns, T.; Lotze, G.; Mayer, J.; Pergushov, D.V.; Plamper, F.A. Facile screening of various micellar morphologies by blending miktoarm stars and diblock copolymers. *ACS Macro Lett.* **2017**, *6*, 711–715. [CrossRef]

11. Dähling, C.; Lotze, G.; Mori, H.; Pergushov, D.V.; Plamper, F.A. Thermoresponsive segments retard the formation of equilibrium micellar interpolyelectrolyte complexes by detouring to various intermediate structures. *J. Phys. Chem. B* **2017**, *121*, 6739–6748. [CrossRef] [PubMed]

12. Nakai, K.; Nishiuchi, M.; Inoue, M.; Ishihara, K.; Sanada, Y.; Sakurai, K.; Yusa, S. Preparation and characterization of polyion complex micelles with phoshobetaine shells. *Langmuir* **2013**, *29*, 9651–9661. [CrossRef] [PubMed]

13. Nakai, K.; Ishihara, K.; Yusa, S. Preparation of giant polyion complex vesicles (G-PICsomes) with polyphosphobetaine shells composed of oppositely charged diblock copolymers. *Chem. Lett.* **2017**, *46*, 824–827. [CrossRef]

14. Nakai, K.; Ishihara, K.; Kappl, M.; Fujii, S.; Nakamura, Y.; Yusa, S. Polyion complex vesicles with solvated phosphobetaine shells formed from oppositely charged diblock copolymers. *Polymers* **2017**, *9*, 49. [CrossRef]

15. Iwasaki, Y.; Ishihara, K. Cell membrane-inspired phospholipid polymers for developing medical devices with excellent biointerfaces. *Sci. Technol. Adv. Mater.* **2012**, *13*, 064101. [CrossRef] [PubMed]

16. Iwasaki, Y.; Ijuin, M.; Mikami, A.; Nakabayashi, N.; Ishihara, K. Behavior of blood cells in contact with water-soluble phospholipid polymer. *J. Biomed. Mater. Res.* **1999**, *6*, 360–367. [CrossRef]

17. Ishihara, K.; Ueda, T.; Nakabayasi, N. Preparation of phospholipid polymers and their properties as hydrogel sheet. *Polym. J.* **1990**, *22*, 355–360. [CrossRef]

18. Ostuni, E.; Chapman, R.G.; Holmlin, R.E.; Takayama, S.; Whitesides, G.M. A survey of structure-property relationships of surfaces that resist the adsorption of protein. *Langmuir* **2001**, *17*, 5605–5620. [CrossRef]

19. Holmlin, R.E.; Chen, X.; Chapman, R.G.; Takayama, S.; Whitesides, G.M. Zwitterionic SAMs that resist nonspecific adsorption of protein from aqueous buffer. *Langmuir* **2001**, *17*, 2841–2850. [CrossRef]

20. Zhao, T.; Chen, K.; Gu, H. Investigations on the interactions of proteins with polyampholyte-coated magnetite nanoparticles. *J. Phys. Chem. B* **2013**, *117*, 14129–14135. [CrossRef] [PubMed]

21. Chang, Y.; Chen, S.; Zhang, Z.; Jiang, S. Highly protein-resistant coatings from well-defined diblock copolymers containing sulfobetaines. *Langmuir* **2006**, *22*, 2222–2226. [CrossRef] [PubMed]

22. Zhang, Z.; Chen, S.; Jiang, S. Dual-functional biomimetic materials: Nonfouling poly(carboxybetaine) with active functional groups for protein immobilization. *Biomacromolecules* **2006**, *7*, 3311–3315. [CrossRef] [PubMed]

23. Muro, E.; Pons, T.; Lequeux, N.; Fragola, A.; Sanson, N.; Lenkei, Z.; Dubertret, B. Small and stable sulfobetaine zwitterionic quantum dots for functional live-cell imaging. *J. Am. Chem. Soc.* **2010**, *132*, 4556–4557. [CrossRef] [PubMed]

24. Shih, Y.; Chang, Y.; Quemener, D.; Yang, H.; Jhong, J.; Ho, F.; Higuchi, A.; Chang, Y. Hemocompatibility of polyampholyte copolymers with well-defined charge bias in human blood. *Langmuir* **2014**, *30*, 6489–6496. [CrossRef] [PubMed]

25. Nakahata, R.; Yusa, S. Solution properties of amphoteric random copolymers bearing pendant sulfonate and quaternary ammonium groups with controlled structures. *Langmuir* **2018**. [CrossRef] [PubMed]

26. Mitsukami, Y.; Donovan, S.M.; Lowe, B.A.; McCormick, L.C. Water-soluble polymers. 81. Direct synthesis of hydrophilic styrenic-based homopolymers and block copolymers in aqueous solution via RAFT. *Macromolecules* **2001**, *34*, 2248–2256. [CrossRef]

27. Koppel, E.D. Analysis of macromolecular polydispersity in intensity correlation spectroscopy: The method of cumulants. *J. Chem. Phys.* **1972**, *57*, 4814–4820. [CrossRef]

28. Huber, K.; Bantle, S.; Lutz, P.; Burchard, W. Hydrodynamic and thermodynamic behavior of short-chain polystyrene in toluene and cyclohexane at 34.5 °C. *Macromolecules* **1985**, *18*, 1461–1467. [CrossRef]

29. Konishi, T.; Yoshizaki, T.; Yamakawa, H. On the "Universal Constants" ρ and Φ. of flexible polymers. *Macromolecules* **1991**, *24*, 5614–5622. [CrossRef]

30. Zimm, H.B. Apparatus and methods for measurement and interpretation of the angular variation of light scattering; Preliminary results on polystyrene solutions. *J. Chem. Phys.* **1948**, *16*, 1099–1116. [CrossRef]

31. Ali, I.S.; Heuts, A.P.J.; van Herk, A.M. Controlled synthesis of polymeric nanocapsules by RAFT-based vesicle templating. *Langmuir* **2010**, *26*, 7848–7858. [CrossRef] [PubMed]

32. Akcasu, A.Z.; Han, C.C. Molecular weight and temperature dependence of polymer dimensions in solution. *Macromolecules* **1979**, *12*, 276–280. [CrossRef]

33. Matsuda, Y.; Kobayashi, M.; Annaka, M.; Ishihara, K.; Takahara, A. Dimensions of a free linear polymer immobilized on silica nanoparticles of a zwitterionic polymer in aqueous solutions with various ionic strength. *Langmuir* **2008**, *28*, 8772–8778. [CrossRef] [PubMed]

34. Cheng, L.; Hou, G.; Miao, J.; Chen, D.; Jiang, M.; Zhu, L. Efficient synthesis of unimolecular polymeric janus nanoparticles and their unique self-assembly behavior in a common solvent. *Macromolecules* **2008**, *41*, 8159–8166. [CrossRef]

35. Savoji, M.T.; Strandman, S.; Zhu, X.X. Switchable vesicles formed by diblock random copolymers with tunable pH-and thermo-responsiveness. *Langmuir* **2013**, *29*, 6823–6832. [CrossRef] [PubMed]

36. Anraku, Y.; Kishimura, A.; Oba, M.; Yamasaki, Y.; Kataoka, K. Spontaneous formation of nanosized unilamellar polyion complex vesicles with tunable size and properties. *J. Am. Chem. Soc.* **2010**, *132*, 1631–1636. [CrossRef] [PubMed]

37. Santis, D.S.; Ladogana, D.R.; Diociaiuti, M.; Masci, G. Pegylated and thermosensitive polyion comples micelles by self-assembly of two oppositely and permanently charged diblock copolymers. *Macromolecules* **2010**, *43*, 1992–2001. [CrossRef]

38. Maggi, F.; Ciccarelli, S.; Diociaiuti, M.; Casciardi, S.; Masci, G. Chitosan nanogels by template chemical cross-linking in polyion complex micelle nanpreactors. *Biomacromolecules* **2011**, *12*, 3499–3507. [CrossRef] [PubMed]